HHS Public Access

Author manuscript

Acta Biomater. Author manuscript; available in PMC 2015 July 09.

Published in final edited form as:

Acta Biomater. 2011 May ; 7(5): 2101–2108. doi:10.1016/j.actbio.2011.01.022.

Elastic fibers in the aortic valve spongiosa: a fresh perspective on its structure and role in overall tissue function

Hubert Tseng and **K. Jane Grande-Allen**

Department of Bioengineering, Rice University, P.O. Box 1892 – MS 142, Houston, TX USA 77251-1892

Abstract

This study characterized the elastic fiber structure within the aortic valve spongiosa, the middle layer of the tri-laminate leaflet. The layer is rich in glycosaminoglycans and proteoglycans, through which it resists compression and lubricates shear between the outer layers. Elastin in this layer forms a fine, interweaving structure, yet it is unclear how this particular structure, which uses elasticity to preload the leaflet, assists spongiosa function. In this study, immunohistochemistry and scanning electron microscopy were used to characterize spongiosa elastin, as well as investigate regional differences in structure. Immunohistochemistry for elastin highlighted an intermediate structure that varied in thickness and density between regions. In particular, the spongiosa elastin was thicker in the hinge and coaptation region than in the belly. Scanning electron microscopy of NaOH-digested leaflets showed a rectilinear pattern of elastic fibers in the hinge and coaptation region, as opposed to a radially oriented stripe pattern in the belly. In conclusion, elastic fibers in the spongiosa connect the two outer layers and vary regionally in structure, while possible playing a role in responding to regionally specific loading patterns.

1. Introduction

The aortic valve functions to maintain unidirectional blood flow between the left ventricle and the systemic circulation. When diseased, the aortic valve is usually replaced with either mechanical or bioprosthetic valves. These replacements typically last 15-20 years and fail in predictable manners; mechanical valves fail through hemolysis and thrombosis [1-3], while bioprosthetic valves fail structurally due to calcification and tissue degeneration [4-7]. Native and replacement valve function is highly dependent on the ability of its three constituent leaflets to withstand a wide array of forces exerted by blood flow and pressure, namely: compression, biaxial tension, and flexure (at the hinge and line of coaptation) in diastole; and high shear in systole. These forces require the aortic valve leaflet to be both strong and durable for the approximately 3×10^9 cardiac cycles over the course of one lifetime.

To this end, the composition and organization of the leaflet extracellular matrix (ECM) are key determinants of material properties and valve function. The leaflet ECM is a laminate

Address correspondence to: K. Jane Grande-Allen, Department of Bioengineering, Rice University, P.O. Box 1892 – MS 142, Houston, TX USA 77251-1892, Phone: +1-(713)-348-3704, Fax: +1-(713)-348-5877, grande@rice.edu.

structure consisting of three primary layers, each defined by its own characteristic matrix composition and role in valvular function [8]. The fibrosa, on the outflow side of the aortic valve, consists of circumferentially oriented collagen fibers that provide tensile strength [9, 10]. The ventricularis is a dense sheet of elastic fibers on the inflow side of the valve that is compliant, and provides elasticity and preload to the leaflet [11-15]. In between the fibrosa and ventricularis is the spongiosa, where glycosaminoglycans (GAGs) and proteoglycans (PGs) are believed to confer flexibility, dampen vibrations from closing, and resist delamination [16-19].

However, the characterization of the leaflet matrix as being comprised of three distinct layers with separate functions belies the reality of a more complex matrix structure, in which the layers of the leaflet and the ECM are interconnected and coupled to facilitate overall tissue function. Indeed, the previously accepted paradigm of collagen as a densely localized in the fibrosa was recently broken with the discovery of a more complex 3D structure of crossing, branching collagen fibers using polarized light microscopy [10]. Our hypothesis is that the major interconnecting component between layers is elastic fibers, which span the thickness of the leaflet. While localized in the ventricularis as a dense sheet, elastic fibers are also present in the other two layers, specifically: (i) as sheaths surrounding collagen in the fibrosa, and (ii) as a spongy three-dimensional network in the spongiosa [11, 12, 20]. Of these forms, the elastic fiber structure in the spongiosa is the least characterized, partly due to the difficulty in isolating its structure from the rest of the leaflet [15]. This structure has been observed during microdissection separating the leaflet [15, 19], with scanning electron microscopy (SEM) [11, 12], micro-computed tomography (micro-CT) [11], immunohistochemistry (IHC) [20], and autofluorescence imaging [21, 22], which all have shown a fine elastic fiber network emanating from the ventricularis and connecting to the fibrosa. However, these qualitative observations did not provide substantial insight into the role of the structure in spongiosa and overall tissue function. It remains relatively unclear how elastic fibers aid the functions of the spongiosa in making the leaflet flexible, vibration dampening, and resistant to delamination [17, 19]. This lack of understanding in the structure-function relationship motivated the study and quantification of this specific elastic fiber structure.

In analyzing elastic fibers in the spongiosa, it is important to put this intermediate structure in the context of elastin in overall leaflet function. Elastic fibers are hypothesized to have multiple roles. First, the compliant elastic fibers permit radial extension, which allows the leaflet to extend in diastole to close the valve [13, 15]. Second, the recoil of elastic fibers contracts the leaflet and its matrix constituents, particularly collagen, to its original unloaded configuration. During diastole when the leaflet extends to close the valve, collagen in the fibrosa begins crimped and folded, and then extends radially through the unfurling of these crimps and folds [15, 19]. This process also involves the rotation of circumferentially oriented collagen fibers towards the radial direction [23]. Elastic fibers use recoil to restore the original shape and orientation of collagen quickly and consistently to open the valve and prepare for the next cycle. This restoration of the collagen configuration is reinforced by the application of compressive preload on the fibrosa by elastic fibers, which uses its recoil to maintain the crimped, folded configuration of the fibrosa [14, 15]. Lastly, elastic fibers bear

load at low strain, which allows the leaflet and collagen to stretch passively before bearing load [13, 19].

Elastic fibers also have secondary roles at the individual layer scale. In the ventricularis, elastic fibers form a smooth dense sheet that promotes laminar flow on the inflow surface during systole, and is the main driver of elastic recoil and preload to open and close the valve [13-15, 17]. Elastic fibers in the fibrosa surround and connect collagen, preserving crimp and folds in the fibrosa [11-13]. All considered, elastic fibers in the spongiosa likely contribute to spongiosa and overall elastic fiber function by: (i) connecting elastic fibers in the ventricularis to collagen in the fibrosa, coupling the mechanics of the two layers and matrix components, while using elastic recoil to exert preload on the fibrosa; (ii) distributing stress between collagen and elastic fibers, particularly at low strains; and (iii) passively allowing relative movement and shear between the outer layers [11, 17, 19].

The goal of this study was to describe the elastic fibers within the spongiosa quantitatively using IHC and SEM and subsequently relate these structural characteristics to regionally varying loading patterns. Given the regional variation in aortic valve loading [24], we analyzed these characteristics in three distinct regions: (i) the hinge, the site of attachment to the aortic wall, which experiences mostly flexure [25, 26]; (ii) the belly, the center of the leaflet, which experiences biaxial tension [23]; and (iii) the coaptation region, where the leaflets meet to close the valve, which experiences both compression and flexure [25]. This examination of regionally specific characteristics will provide further insight into the functional role of elastic fibers.

2. Materials and Methods

2.1. Tissue harvest

Fresh porcine hearts were obtained from a local abattoir (Fisher Ham and Meats, Spring, TX) within 3-6 hours of death. Aortic valve leaflets were dissected from the hearts and rinsed in phosphate buffered saline (PBS, pH∼7.4). For IHC and histology, leaflets were fixed in an unloaded state overnight in 10% formalin. For SEM, samples were stored frozen in PBS at -20°C until further use.

2.2. Immunohistochemistry and histology

All leaflets fixed overnight in formalin were subsequently dehydrated and embedded in paraffin according to standard procedures. In order to localize this elastic fiber structure and study its regional variability, leaflets were sectioned either circumferentially or radially (Fig. 1).

Circumferential sections were cut tangential to the hinge in five positions around the annulus: left, left center, center, right center and right (n=9 per position). Radial sections were cut from the center of the free edge to the hinge in five identically termed angular positions: left, left center, center, right center, and right (n=9 per position). Radial sections included the attached aortic root wall in addition to the leaflet, in order to view the elastin and ECM of the hinge in its entirety. Sections were further separated by leaflet type: left, right, and non-coronary.

Immunohistochemical staining was then performed to localize elastin. Antigen retrieval was performed using a chymotrypsin solution (0.1% chymotrypsin, Sigma-Aldrich, St. Louis, MO, 0.1% $CaCl_2$ in dI H_2O, pH∼7.8) for 30 min at 80°C. All sections were blocked using 10% goat serum buffer (GSB, 10% goat serum in PBS, MP Biomedicals, Solon, OH) in PBS. Experimental sections were stained with mouse anti-elastin antibodies (Abcam, Cambridge, MA) at a 1:150 dilution with 1% bovine serum albumin (BSA) in PBS. Negative controls were left to incubate with 10% GSB at this step. All sections were then washed in PBS and incubated with a secondary antibody (biotin-conjugated goat anti-mouse IgG+IgM, Jackson ImmunoResearch, West Grove, PA) at a 1:1000 dilution. Sections were again washed in PBS and followed by the application of an avidin-biotinylated peroxidase solution (Vectastain Elite ABC Kit, Vector Labs, Burlingame, CA). Positive staining was detected using 3,3′-diaminobenzidine (DAB, DAB Peroxidase Substrate Kit, Vector Labs), which stained sections brown. Hematoxylin was used as a counterstain for cell nuclei, which stained purple. In addition, each sample was stained using Movat's pentachrome stain to demonstrate the overall distribution of collagen (yellow), elastic fibers (black), PGs/GAGs (blue), and cells (purple) within the leaflet sections. Images of the section were taken using a charge coupled device (CCD) camera (Leica DFC 320, Leica Microsystems, Bannockburn, IL) connected to an upright microscope (Leica DM LS2, Leica) using image capture software (ImagePro, Media Cybernetics, Bethesda, MD).

The intensity of the elastin IHC stain was measured from duplicate stained sections to quantify density; lower intensity, or darker, regions indicated a denser elastin structure, whereas higher intensity, or lighter, regions indicated a more porous structure. The average intensity within the spongiosa was measured using ImageJ image processing software (NIH, Bethesda, MD) (Fig. 2).

The layers of the leaflet were distinguished from each other by the use of the Movat's stain as a reference, which stains the layers distinctly based on extracellular matrix; the collagenous fibrosa stains yellow/green; the ventricularis, dense with elastic fibers, stains black; and the spongiosa, with its high PG and GAG content, stains blue from Alcian Blue [16, 20]. In order to reduce section-to-section variability in elastin staining, each raw intensity value of elastin in the spongiosa was also normalized to the stain intensity of elastin from the ventricularis, which is always dense in elastin. Variability in normalized intensity values should thus represent true differences in elastin intensity. Intensity was measured for both circumferential and radial sections, although for radial sections, intensity was measured at three locations along the length of the section: the belly, coaptation region, and hinge (Fig. 1). In the belly, the thickness was taken in flat areas, which is a more commonly associated with the region. In addition, the thickness of the spongiosa of radial sections was measured in pixels as a percentage of overall leaflet thickness using ImageJ (Fig. 2).

2.3. Scanning electron microscopy

Leaflets were digested in 0.1 N NaOH at 75°C for at least 45 minutes, a method previously used to isolate elastic fibers by dissolving other ECM [11-13]. A Delrin jig was used to clamp the leaflet during digestion to prevent elastic fibers from curling, as Delrin could

withstand NaOH digestion, and would allow for frictionless removal of digested leaflets. Leaflets were subsequently frozen in -80°C for at least 20 minutes, lyophilized overnight, and removed from the jig. A notably light structure appeared on top of the leaflet, which was assumed to be elastic fibers from the fibrosa, and was gently brushed aside, leaving elastic fibers in the spongiosa and ventricularis for imaging. Leaflets were then cut in half radially (from the center of the free edge to the hinge) and mounted onto microscope stubs with the spongiosa facing upwards. These samples were then sputter coated with gold (CRC-150 Sputter Coater, Torr International, Windsor, NY) and imaged using the SEM (Quanta 400, FEI, Hillsboro, OR). Images were taken at the hinge, belly, and coaptation regions (n=14 images per region) at 250× magnification with a resolution of 1024×768 in 8-bit grayscale.

The elastic fiber network properties were measured from the SEM images using custom image analysis software written with the Image Processing Toolbox in MATLAB (Mathworks, Natick, MA). Images of the hinge and coaptation region showed elastic fibers that were rectilinear in pattern, so for these images, the area of the voids between elastic fibers was measured. After converting images to black and white and inverting, the voids were labeled and sized using the *bwlabel* function, with voids less than 144 pixels in size regarded as noise and ignored. All void areas were then averaged over the whole image. For belly images, the elastic fibers demonstrated a striped pattern, so the distance between stripes was measured. The overall direction of elastic fibers in these grayscale images was measured using an edge detection algorithm that was previously used to determine myofiber and electrospun fiber orientation [27-29]. Briefly, the algorithm used 11×11 (s=5) vertical and horizontal masks with σ=2.5 [27]. An accumulator weight function was then used to find the dominant angular orientation of the elastic fibers [28]. Afterwards, these images were converted to black and white and objects less than 144 pixels in area were labeled and deleted using *bwlabel*. The horizontal distance between stripes was calculated by scanning across the image at a particular row and measuring between stripes. Rows 192, 384, 576 were used, or one-quarter, one-half, and three-quarters down the image height, respectively. Using the angle found through edge detection, the minimum distance between stripes was found. All distances calculated were averaged for the entire image.

2.4. Statistical Analysis

All data was analyzed using statistical analysis software (SigmaStat, SPSS, Chicago, IL) for single and multiple factor ANOVAs. Significance was defined as $p<0.05$. If a significant difference was observed, post-hoc testing was conducted using Tukey's test to observe pairwise comparisons. All values are presented as mean ± standard deviation.

3. Results

3.1. Immunohistochemistry

Immunohistochemistry revealed a layered distribution of elastin that matched the layered structure of the aortic valve matrix as observed in Movat's stains with little to no intensity staining in the fibrosa, light staining in the spongiosa, and a strong staining of elastic fibers in the ventricularis. In the spongiosa of all sections, elastin appeared sponge-like in

structure, forming a finely fibrous, interwoven, porous network that extended from the ventricularis to the fibrosa.

Circumferential sections of the hinge were uniformly thick and showed the interwoven elastin structures within the spongiosa at each position (Fig. 3).

There was no significant difference in intensity of elastin staining in the spongiosa relative to the ventricularis as a result of either position around the annulus or leaflet type (i.e., left, right, or non-coronary). The intensity value of elastin staining was on average 128.71±18.92, or 1.23±0.21 times larger than the intensity value of the ventricularis across all positions and leaflet type.

The radial sections showed distinct spongiosa elastin structures that varied in thickness throughout the leaflet length, whereas the two outer layers were observed to have a consistent thickness at the three regions of interest (Fig. 4).

At the hinge, the spongiosa originated from the medial layer of the aortic wall as a thick layer that gradually decreased in thickness moving towards the belly. In the belly, the spongiosa was mostly flat, although there were rare instances, particularly in the center, where collagen bundles crossed and formed characteristic corrugated structures, underneath which elastin emanated from the ventricularis and branched out to connect to the fibrosa (Fig. 5).

Moving towards the coaptation region, the spongiosa increased in thickness once again. There was a significant regional difference in relative spongiosa thickness ($p<0.001$), with the belly (27.97±8.25%) having significantly lower relative thickness than both the hinge (43.69±13.35%) and coaptation region (39.52±11.27%, $p<0.001$ for both, Fig. 6).

There was no regional difference in relative stain intensity. There was no significant difference found in relative intensity and thickness based on either the angle at which it was sectioned or type. The intensity value of elastin staining was on average 129.53±18.63, or 1.45±0.35 times larger than the intensity value of the ventricularis across all angles, regions and leaflet type.

3.2. Scanning electron microscopy

Scanning electron microscopy revealed two distinct patterns of elastic fibers when examining at the hot alkali digested leaflet with the ventricularis facing down (Fig. 7). Both in the hinge and the coaptation region, a rectilinear structure with rectangular voids was observed. The sides of these voids were oriented radially and circumferentially. Image analysis found that these voids in the rectilinear pattern were statistically similar in the hinge and coaptation regions with an average area in both regions of 446.29±205.80 μm^2. In the belly, elastic fibers mainly formed a radially oriented stripe pattern with fewer, fainter perpendicular struts that crossed from fiber to fiber. The distance between the observed stripes was on average 19.66 ± 3.81 μm. In some areas of the belly, there were small regions patterned with a rectilinear pattern similar to the hinge and coaptation region.

4. Discussion

The goal of this study was to quantify specific characteristics of elastic fibers in the spongiosa using IHC and SEM, and to relate regional differences in structure to loading patterns. This structure has only previously been qualitatively described in simple observations during dissection [15, 19], using SEM [11, 12], micro-CT [11], IHC [20], and autofluorescence imaging [21, 22]. This was the first investigation to date focused on elastic fibers in the spongiosa. The main finding of this study was that elastic fibers in the spongiosa form a finely fibrous, interweaving network that varies regionally in structure. IHC staining of radial sections of the leaflet showed that the thickness of the spongiosa positively staining for elastin was significantly thicker in the hinge and coaptation region than in the belly. The percentage thicknesses measured are consistent with previous measurements of spongiosa thickness (30% [19] and 57% [30]), although these values did not take regionally variable thicknesses into account. There was no difference in elastin stain intensity with respect to both angular position and region. Circumferential sections also showed no difference in elastin stain intensity with respect to position around annulus, which suggests that elastin is equally dense throughout the leaflet. SEM showed two distinct patterns of spongiosa elastic fibers within the leaflet: (i) a rectilinear pattern in the hinge and coaptation region; and (ii) a radially oriented stripe pattern in the belly. These observations were not entirely exclusive to specific regions; there were rare instances observed in IHC where the belly was corrugated rather than flat. These corrugations are formed by collagen bundles that traverse the leaflet circumferentially [15]. Underneath these corrugations, elastin branched out of the ventricularis to connect the two outer layers. In addition, some parts of the belly imaged using SEM had a rectilinear pattern similar to the hinge and coaptation region. As these two structures are present together in the hinge and coaptation region, it is speculated that these two parts are colocalized, and that the rare elastin branching in the belly has similar functionalities to that of the thicker spongiosa in the hinge and coaptation regions.

These results add to the larger picture of elastin in the leaflet. In previous studies using SEM to describe the elastic fibers in the separated layers of the leaflet, elastic fibers were found to form a loose structure that formed sheaths around collagen, while the separated ventricularis formed dense sheets [11, 12]. In this study, we have analyzed an intact elastic fiber structure in a layer that is ignored when the leaflet is separated, as well as looked at regional differences in structure. The overall result is a combined picture of how elastin exists in the leaflet that allows us to speculate about the relationship between elastin and regionally specific loading.

4.1. Thicker, rectilinear elastin in the spongiosa in the hinge and coaptation region

Given the presence of a thick structure of elastic fibers in the spongiosa with a rectilinear pattern in the hinge and coaptation region, areas associated with bending, we speculate that this elastin structure plays a role in flexing the leaflet. This correlation is consistent with previously published speculation that elastic fibers and the spongiosa aid in flexing the leaflet [15, 17]. When the leaflet flexes towards the outflow direction, the fibrosa is compressed and the ventricularis pulls in tension. Rather than compressing, however, the

fibrosa may attempt to buckle separately from the leaflet, thereby exaggerating its “peaks and troughs” configuration. The leaflet would subsequently bend at these troughs, where the second moment of inertia would be lowered temporarily. Buckling would only occur with shearing between the fibrosa and ventricularis, which is allowed by both the compliant elastic fibers in the spongiosa connecting the two outer layers as well as by GAGs in the spongiosa lubricating the outer layer movement [15, 17, 31, 32]. Recoil from elastic fibers in the spongiosa would then return the fibrosa to its original configuration in preparation of the next cycle [15, 17]. This theory is supported by studies showing that glutaraldehyde-treated leaflets, which over time lose GAGs and water, and are therefore devoid of a spongiosa structure, are stiffer in both bending and shear [31-34]. At the hinge, where bending occurs in the opposite direction, we speculate that the ventricularis likely compresses readily without buckling, most likely due to the tensile preload already exerted on the ventricularis, but that leaflet deflection may be limited by the stiff fibrosa, which won't allow the leaflet to bend [14, 35]. Limited flexure at the hinge would likely allow the leaflet to absorb pressure from reverse blood flow in diastole, but prevents distention of the leaflet. Thus, the finding of a thicker spongiosa and elastic fiber structure in flexural regions, in combination with previous mechanical studies on elastin in the leaflet, serves as further evidence of a significant role for elastin in flexure.

In addition, the thick spongiosa observed in the coaptation region possibly plays a role for both GAGs and elastic fibers of the layer in leaflet compression. This layer is believed to dampen vibrations from valve closing, requiring the layer to have low compressive stiffness and be viscoelastic [17]. The thicker, more hydrated GAG-rich matrix seen in this region would likely yield the necessary compressive properties. Thus, a thicker spongiosa elastic fibers structure may have a role in dampening vibrations from leaflet closing.

However, the rectilinear pattern of voids in the hinge and coaptation regions, with their sides oriented radially and circumferentially, does not easily reflect the flexibility of these regions. Radially, the leaflet bends and extends to close the valve and withstand retrograde pressure from blood in the aorta. These forces acting in this direction would necessitate the presence of radially oriented elastic fibers for rapid recoil during systole. However, the circumferentially oriented elastic fibers are not easily explained, as the leaflet does not stretch circumferentially as easily as it does radially [36]. The presence of this rectilinear pattern merits further investigation into its contribution to overall leaflet mechanics.

4.2. Thinner spongiosa and spongiosa elastin in belly

Within the belly spongiosa, a thin, a radially oriented elastic fiber structure was found. It has been previously hypothesized that the primary role of elastin is to preload the outer layers [14, 15], and we speculate that elastic fibers in this region follow that role. A thinner, loose elastic fiber structure in the spongiosa would not permit the amount of relative movement and shearing between the ventricularis and fibrosa that would be needed for flexure or compression, due to the lack of GAGs. Thus, the main function of elastic fibers of the spongiosa in the belly would most likely be to connect the two outer layers and to use recoil and preload to restore collagen to its original configuration. This speculated function is similar to a another hypothesis that the spongiosa in the belly simply resists delamination

during biaxial tension [19]. We speculate that the radial orientation of the striped pattern may reflect the extension of the leaflet in that direction, and the need to open the valve, as well as preserve radially oriented corrugations in the fibrosa. These observations of elastic fibers of the spongiosa in the belly provide a larger picture of their presence and likely function in the leaflet.

4.3. Limitations

These results should be interpreted in light of some study limitations. First, with regards to digesting the leaflet in NaOH, it was assumed the porous structure atop the leaflet was comprised of elastic fibers from the fibrosa, which was therefore removed after lyophilization of the digested leaflet [11, 12]. As discussed, it is likely that elastic fibers of the spongiosa play a key role in connecting the two outer layers. In removing these fibers, the connections between elastic fibers in the spongiosa and in the fibrosa were ignored, but removing this structure was necessary to image the elastic fibers in the spongiosa. While this interface was not explored in more detail due to the frailty of the structures involved, future studies should attempt to preserve and study this interface. Secondly, the leaflets for SEM image were frozen prior to lyophilization at -80°C for at least 20 min in order to freeze water. The freezing procedure can have a significant effect on tissue size and porosity, although leave general tissue structure intact [37]. Thus, even as each leaflet was frozen similarly, it is possible that tissue morphology was affected. Thirdly, excising the valve from the heart involves the release of residual strains, which is manifested in the contraction of ventricularis and could affect elastic fiber structure [19]. This could have affected circumferential sections, which were taken from leaflets excised out of the heart before fixation, but only intensity was measured and nothing structural. In radial IHC sections, where thickness was measured, the leaflet was excised along with the aortic wall, and cut only after fixation, when it would have a much smaller effect on tissue structure. Fourthly, the use of IHC and SEM did not provide a full three-dimensional perspective of the leaflet. This study simply reconstructed such a view from two orthogonal views using two wholly different methods. To view the structure in its entirety, non-destructive imaging methods such as autofluorescence imaging may be useful in future studies [21, 22]. Lastly, the purpose of this study was to view and characterize elastin within the leaflet, and regional structural differences found were correlated with known regional loading patterns. However, such relationships between elastin structure and loading would ideally be conducted in an experimental framework involving nondestructive, direct visualization of elastin during mechanical testing. Thus, the proposed theories regarding elastic fibers in the spongiosa and their regionally-specific roles is only speculative.

5. Conclusion

Although previous studies have observed an elastic fiber structure within the spongiosa, none have characterized it in a quantitative manner, nor considered regional differences and their relationship to heterogeneous loading experienced by aortic valve leaflets. This study measured the thickness, density, and spacing of this intermediate structure, and interpreted these regionally varying structures in the context of tissue mechanics and function both at

the regional and global levels. The findings presented here help to provide a more complete picture of extracellular matrix structure within the aortic valve leaflet.

Acknowledgments

The study presented was funded in part by the American Heart Association South Central Affiliate Grant-in-Aid, 09GRNT2220150, and NIH 5T32 GM008362. The authors would also like to thank Daniel Gould, Baylor College of Medicine, for help in image processing, and Richard Thibault and Angelo Benedetto, Rice University, for help with SEM.

References

1. Metzdorff M, Grunkemeier G, Pinson C, Starr A. Thrombosis of mechanical cardiac valves: a qualitative comparison of the silastic ball valve and the tilting disc valve. J Am Coll Cardiol. 1984; 4:50–3. [PubMed: 6736454]
2. Grunkemeier G, Rahimtoola S. Artificial heart valves. Annu Rev Med. 1990; 41:251–63. [PubMed: 2184728]
3. Hylen J. Mechanical malfunction and thrombosis of prosthetic heart valves. Am J Cardiol. 1972; 30:394–404.
4. Binet J, Carpentier A, Langlois J. Clinical use of heterografts for replacement of the aortic valve. J Thorac Cardiovasc Surg. 1968; 55:238–42. [PubMed: 5688789]
5. Kloevekorn W, Meisner H, Paek S, Sebening F. Long-term results after right ventricular outflow tract reconstruction with porcine bioprosthetc conduits. J Card Surg. 1991; 6:624–6. [PubMed: 1810557]
6. Schoen F. Cardiac valve prostheses: pathological and bioengineering considerations. J Card Surg. 1987; 21:65–108. [PubMed: 2979963]
7. Korossis S, Fisher J, Ingham E. Cardiac valve replacement: A bioengineering approach. Biomed Mater Eng. 2000; 10:83–124. [PubMed: 11086842]
8. Gross L, Kugel M. Topographic anatomy and histology of the valves in the human heart. Am J Pathol. 1931; 7:445–56. [PubMed: 19969978]
9. Sacks M, Smith D, Hiester E. The aortic valve microstructure: effects of transvalvular pressure. J Biomed Mater Res. 1998; 41:131–41. [PubMed: 9641633]
10. Doehring T, Kahelin M, Vesely I. Mesostructures of the aortic valve. J Heart Valve Dis. 2005; 14:679–86. [PubMed: 16245508]
11. Scott M, Vesely I. Aortic valve cusp microstructure: the role of elastin. Ann Thorac Surg. 1995; 60:S391–4. [PubMed: 7646194]
12. Scott M, Vesely I. Morphology of porcine aortic valve cusp elastin. J Heart Valve Dis. 1996; 5:464–71. [PubMed: 8894984]
13. Vesely I. The role of elastin in aortic valve mechanics. J Biomech. 1998; 31:115–23. [PubMed: 9593204]
14. Vesely I, Lozon A. Natural preload of aortic valve leaflet components during glutaraldehyde fixation: effects on tissue mechanics. J Biomech. 1993; 26:121–31. [PubMed: 8429055]
15. Vesely I, Noseworthy R. Micromechanics of the fibrosa and the ventricularis in aortic valve leaflets. J Biomech. 1992; 25:101–13. [PubMed: 1733978]
16. Stephens E, Chu C, Grande-Allen K. Valve proteoglycan content and glycosaminoglycan fine structure are unique to microstructure, mechanical load and age: Relevance to an age-specific tissue-engineered heart valve. Acta Biomater. 2008; 4:1148–60. [PubMed: 18448399]
17. Schoen F. Aortic valve structure-function correlations: role of elastic fibers no longer a stretch of the imagination. J Heart Valve Dis. 1997; 6:1–6. [PubMed: 9044068]
18. Deck J, Thubrikar M, Schneider P, Nolan S. Structure, stress, and tissue repair in aortic valve leaflets. Cardiovasc Res. 1988; 22:7–16. [PubMed: 3167931]
19. Stella J, Sacks M. On the biaxial mechanical properties of the layers of the aortic valve leaflet. J Biomech Eng. 2007; 129:757–66. [PubMed: 17887902]

20. Latif N, Sarathchandra P, Taylor P, Antoniw J, Yacoub M. Localization and pattern of expression of extracellular matrix components in human heart valves. J Heart Valve Dis. 2005; 14:218–27. [PubMed: 15792183]
21. Konig K, Schenke-Layland K, Riemann I, Stock U. Multiphoton autofluorescence imaging of intratissue elastic fibers. Biomaterials. 2005; 26:495–500. [PubMed: 15276357]
22. Christov A, Liu L, Lowe S, Icton C, Dunmore-Buyze J, Boughner D, et al. Laser-induced fluorescence (LIF) recognition of the structural composition of porcine heart valves. Photochem Photobiol. 1999; 69:382–9. [PubMed: 10089832]
23. Billiar K, Sacks M. Biaxial mechanical properties of the natural and glutaraldehyde-treated aortic valve cusp: Part I - Experimental results. J Biomech Eng. 2000; 122:23–30. [PubMed: 10790826]
24. Lo D, Vesely I. Biaxial strain analysis of the porcine aortic valve. Ann Thorac Surg. 1995; 60:S374–8. [PubMed: 7646191]
25. Thubrikar M, Aouad J, Nolan S. Patterns of calcific deposits in operatively excised stenotic or purely regurgitant aortic valves and their relation to mechanical stress. Am J Cardiol. 1986; 58:304–8. [PubMed: 3739919]
26. Misfeld M, Sievers H. Heart valve macro- and microstructure. Philosophical Transactions of the Royal Society of London Series B, Biological Sciences. 2007; 362:1421–36.
27. Chaudhuri B, Kundu P, Sarkar N. Detection and gradation of oriented texture. Pattern Recognit Lett. 1993; 14:147–53.
28. Karlon W, Covell J, McCulloch A, Hunter J, Omens J. Automated measurement of myofiber disarray in transgenic mice with ventricular expression of ras. Anat Rec. 1998; 252:612–25. [PubMed: 9845212]
29. Courtney T, Sacks M, Stankus J, Guan J, Wagner W. Design and analysis of tissue engineering scaffolds that mimic soft tissue mechanical anisotropy. Biomaterials. 2006; 27
30. Merryman W, Huang H, Schoen F, Sacks M. The effects of cellular contraction on aortic valve leaflet flexural stiffness. Journal of Biomechanics. 2006; 39:88–96. [PubMed: 16271591]
31. Talman E, Boughner D. Glutaraldehyde fixation alters the internal shear properties of porcine aortic heart valve tissue. Ann Thorac Surg. 1995; 60:S369–73. [PubMed: 7646190]
32. Talman E, Boughner D. Effect of altered hydration on the internal shear properties of porcine aortic valve cusps. Ann Thorac Surg. 2001; 71:S375–8. [PubMed: 11388228]
33. Grande-Allen K, Mako W, Calabro A, Shi Y, Ratliff N, Vesely I. Loss of chondroitin 6-sulfate and hyaluronan from failed procine bioprosthetic valves. J Biomed Mater Res A. 2003; 65:251–9. [PubMed: 12734820]
34. Vesely I, Boughner D. Analysis of the bending behaviour of porcine xenograft leaflets and of natural aortic valve material: bending stiffness, neutral axis and shear measurements. J Biomech. 1989; 22:655–71. [PubMed: 2509479]
35. Vesely I, Boughner D. Tissue buckling as a mechanism of bioprosthetic valve failure. Ann Thorac Surg. 1988; 46:302–8. [PubMed: 3137903]
36. Lee J, Courtman D, Boughner D. The glutaraldehyde-stabilized porcine aortic valve xenograft. I. Tensile viscoelastic properties of the fresh leaflet material. Journal of Biomedical Materials Research. 1984; 18:61–77. [PubMed: 6699033]
37. Curtil A, Pegg D, Wilson A. Freeze drying of cardiac valves in preparation for cellular repopulation. Cryobiology. 1997; 34:13–22. [PubMed: 9028913]

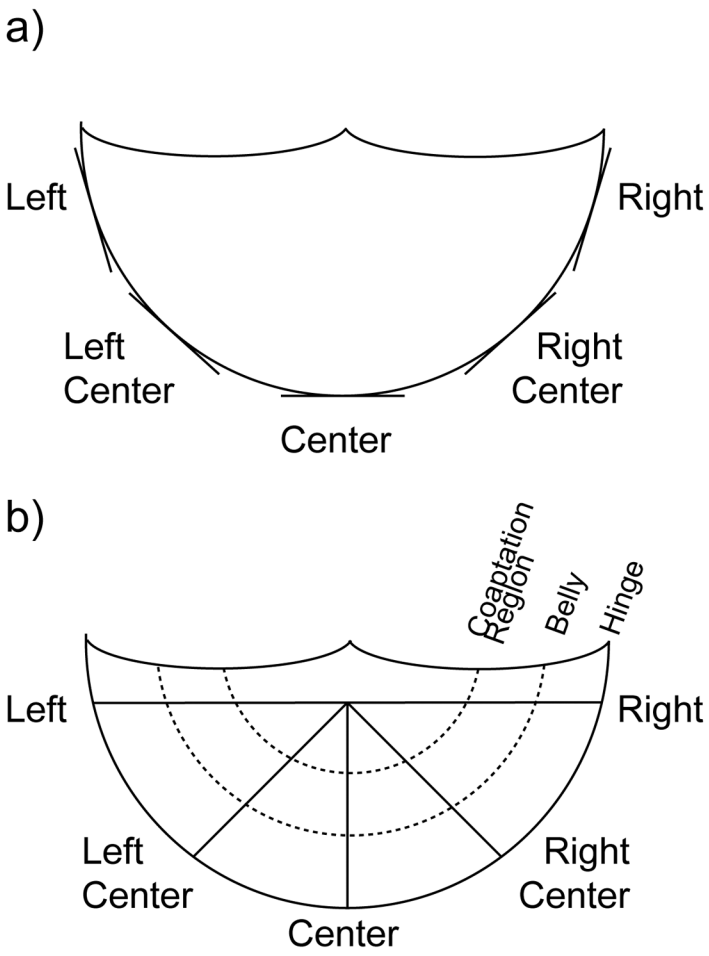

Figure 1.

Schematic of sections cut for IHC and histology. Circumferential sections were cut along the annulus. Radial sections were cut from the center of the free edge to the annulus. Within radial sections, the elastic fiber structure in three regions was analyzed: hinge, belly, and coaptation region.

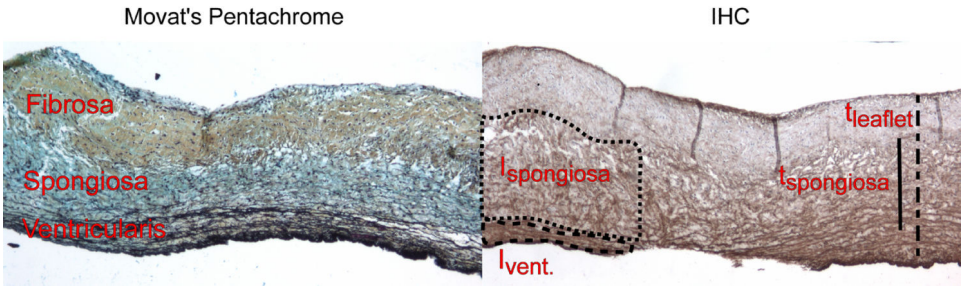

Figure 2.

Examples of Movat's pentachrome (collagen=yellow, PGs/GAGs=blue, elastin=black, cell nuclei=purple) and elastin IHC (elastin=brown, cell nuclei=purple) stains of heart valve leaflets. The separate layers of the leaflet can be distinguished by the matrix stain in Movat's: the fibrosa is mostly yellow from collagen; the spongiosa is blue with GAGs/PGs; and the ventricularis contains fine black elastic fibers. Using the Movat's stain as a reference, thickness and intensity were measured as pictured on the right.

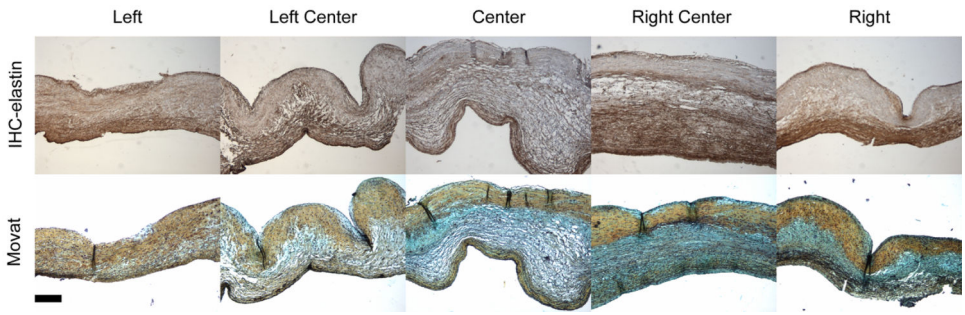

Figure 3.

Elastin IHC (elastin=brown, cell nuclei=purple) and Movat's pentachrome stains (collagen=yellow, PGs/GAGs=blue, elastin=black, cell nuclei=purple) for circumferential sections. IHC revealed a fine, interweaving elastin structure in the spongiosa that matched the strong blue stain of GAGs in the Movat's stains. Scale bar=200 μm.

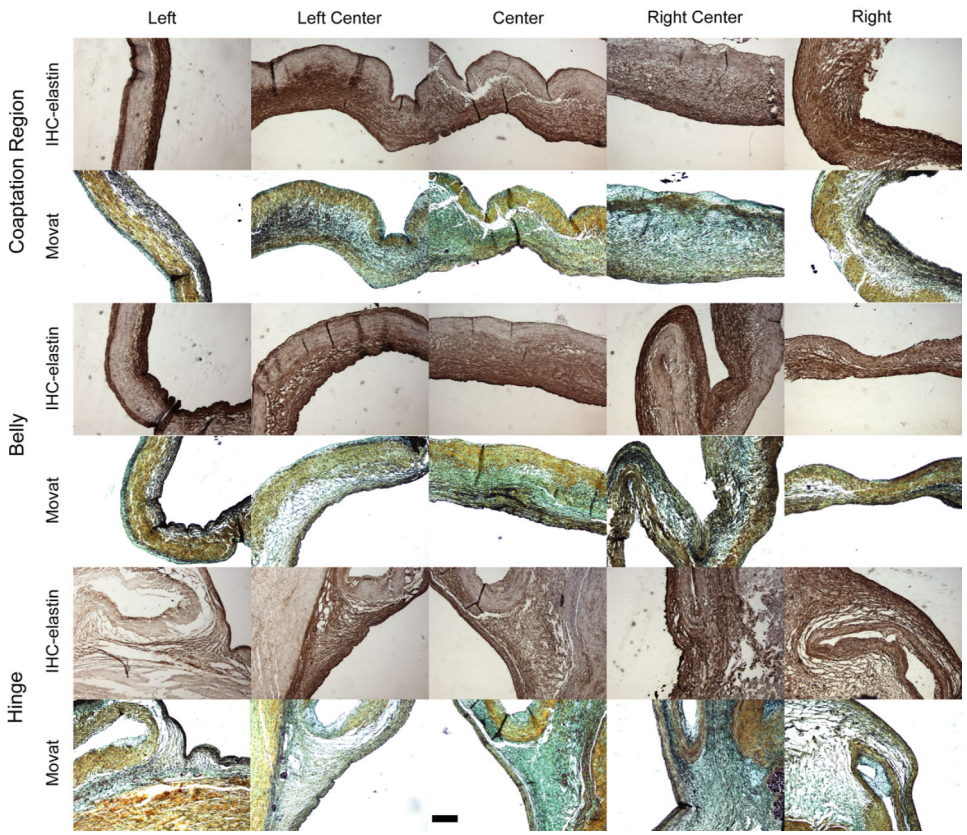

Figure 4.

Elastin IHC (elastin=brown, cell nuclei=purple) and Movat's pentachrome stains (collagen-yellow, PGs/GAGs=blue, elastin=black, cell nuclei=purple) for radial sections at three regions: hinge, belly, and coaptation region. In the hinge, the spongiosa elastin structure started thick and gradually decreased in thickness when moving towards the belly, where it was thinnest. Spongiosa elastin increased again in thickness towards the coaptation region. Scale bar=200 μm.

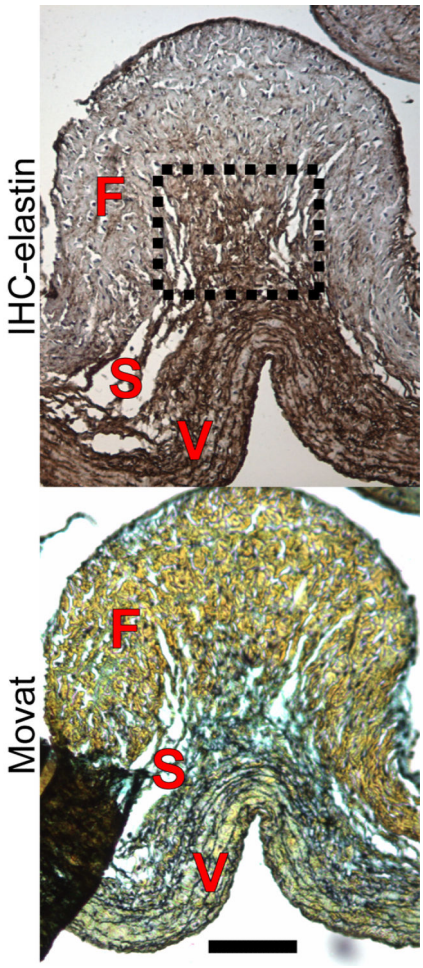

Figure 5.

Elastin IHC (elastin=brown, cell nuclei=purple) and Movat's pentachrome stains (collagen-yellow, PGs/GAGs=blue, elastin=black, cell nuclei=purple) of a collagen fold in the belly, taken from a center section. Whereas the spongiosa was thin through the majority of the belly, underneath collagen folds such as this one, elastin emanated from the ventricularis and branched out to connect the fibrosa. Scale bar=100 μm.

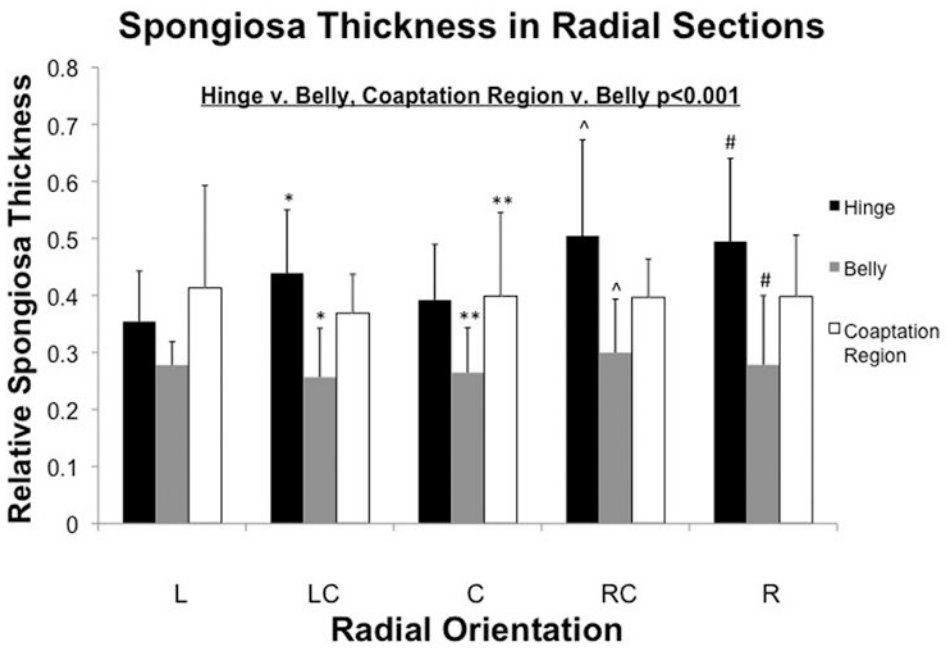

Figure 6.

Thickness of spongiosa elastin normalized to the whole leaflet. There was a significant regional effect in spongiosa thickness ($p<0.001$), with significant differences found between the hinge and belly, and between the coaptation region and belly ($p<0.05$). Pairwise differences within angular positions are shown. (*:$p<0.05$)

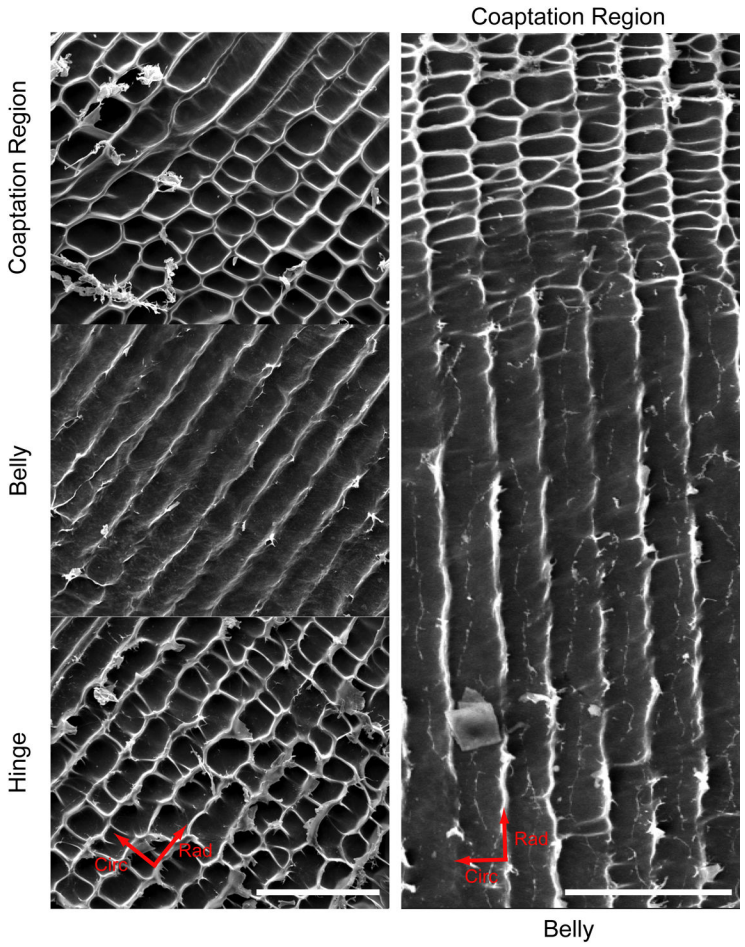

Figure 7.

SEM images of NaOH-digested leaflets at the hinge, belly, and coaptation regions on the left at 250× magnification, and the hinge and belly on the right at 50× magnification. Elastic fibers formed rectilinear patterns in the hinge and coaptation regions, and a radially oriented striped pattern in the belly. Note the organized structure and smooth transition between regions on the right. Scale bar=200 μm.